Dye removal from aqueous solution by raw maize corncob and H_3PO_4 activated maize corncob

M. Farnane, H. Tounsadi, A. Machrouhi, A. Elhalil, F. Z. Mahjoubi, M. Sadiq, M. Abdennouri, S. Qourzal and N. Barka

ABSTRACT

The focus of this study is the investigation of removal ability of methylene blue (MB) and malachite green (MG) dyes from aqueous solution by raw maize corncob (RMC) and H_3PO_4 activated maize corncob (AMC). Maize corncobs were carbonized at 500 °C for 2 h, and then impregnated at a phosphoric acid to maize corncob ratio of 2.5 g/g. The impregnated maize corncob was activated in a tubular vertical furnace at 450 °C for 2 h. Samples were characterized by different methods. Adsorption experiments were carried out as a function of solution pH, adsorbent dosage, contact time, initial concentration of dyes and the temperature. Experimental results show that the activation of maize corncob boosts four times the adsorption performance for the selected dyes. The adsorption process is very rapid and was pH dependent with high adsorption capacities in the basic range. The kinetic data were fitted with the pseudo-second-order kinetic model. The best fit of equilibrium data was obtained by the Langmuir model with maximum monolayer adsorption capacities of 75.27 and 271.19 mg/g for MB, 76.42 and 313.63 mg/g for MG, respectively, in the case of RMC and AMC. The temperature did not have much influence on the adsorption performance.

Key words | activated corncob, dye removal, textile wastewater

M. Farnane
H. Tounsadi
A. Machrouhi
A. Elhalil
F. Z. Mahjoubi
M. Sadiq
M. Abdennouri
N. Barka (corresponding author)
Laboratoire des Sciences des Matériaux,
des Milieux et de la Modélisation (LS3M), FPK,
Univ Hassan 1, B.P. 145,
Khouribga 25000,
Morocco
E-mail: *barkanoureddine@yahoo.fr*

S. Qourzal
Equipe de Catalyse et Environnement,
Département de Chimie, Faculté des Sciences,
Université Ibn Zohr,
Cité Dakhla B.P. 8106,
Agadir,
Morocco

INTRODUCTION

Water is the most important raw material for human beings, animals, plants, and micro-organisms. Virtually all vital phenomena of the biosphere are related to the availability of water. Due to the rapid development in technology, water pollution is a major problem being faced by society today. The discharge of industrial, agricultural, and domestic wastewaters without treatment or with inadequate treatment level causes degradation of ecosystems (Vymazal 2014). The problem is even more serious in the case of industrial effluents which have a much more pronounced toxic nature.

Among industries consuming water in large quantities, the textile industry with that of tanneries came top of the list (Patterson 2012). The dyeing sector, and printing and finishing of textiles are of particular importance (Wang *et al.* 2011; Rosa *et al.* 2014). These activities generate a significant pollution in wastewater being highly loaded with acidic or basic dyes, salts, and adjuvants (Secondes *et al.* 2014). Disposal of these dyes has been extensively studied, with the processes used including precipitation (Zhu *et al.* 2007), ionic exchange (Greluk & Hubicki 2011), membrane filtration (Zylla *et al.* 2006), electrochemical destruction (Lin & Peng 1996; Brillas & Martinez-Huitle 2015), photodegradation (Barka *et al.* 2011b; Rosa *et al.* 2015; Morikawa & Shinohara 2016), and adsorption (Barka *et al.* 2006; Elmoubarki *et al.* 2015). Among these processes, adsorption is considered as a superior technique comparatively with other treatment

doi: 10.2166/wrd.2017.179

methods due to the availability of many adsorbents, simplicity of design, high efficiency, and ability to treat dyes in a more concentrated form (Kanchi *et al.* 2013; Yagub *et al.* 2014).

Different sorbents have been conventionally used for the removal of dyes from aqueous solutions, whereas activated carbon has been widely used in the recent past due to the presence of different surface oxygen functional groups at its surface, its pore structure, and also for the high adsorption capacity (Titirici *et al.* 2012; Chen *et al.* 2013). The properties of the activated carbons depend on the activation process and the nature of the precursor (Herawan *et al.* 2013; Ranjithkumar *et al.* 2014). Several biomasses have been tested as precursors in the production of activated carbon, including buriti shells (*Mauritia flexuosa* L.) (Junior *et al.* 2014a), waste tea (Gokce & Aktas 2014), hazelnut husk (Karacetin *et al.* 2014), coconut shell (Isah *et al.* 2015), *Diplotaxis harra* (Tounsadi *et al.* 2015), macadamia nut endocarp (*Macadamia integrifolia*) (Junior *et al.* 2014b), olive stones (Hazzaa & Hussein 2015), chlorella-based algal residue (Chang *et al.* 2015), rice husk residue (Li *et al.* 2016), coconut shells and corn cobs (Ensuncho-Munoz & Carriazo 2014). However, studies in this field have not produced materials which meet all the demands of adsorption activity.

This work aims to evaluate the potential of maize corncob and H_3PO_4 activated maize corncob (AMC) as an economical and eco-friendly adsorbent for the removal of methylene blue (MB) and malachite green (MG) from aqueous solution. The materials were characterized by Fourier transform infrared spectroscopy (FT-IR), X-ray diffraction (XRD) and scanning electron microscopy (SEM). Several parameters that affect the adsorption including solution pH, adsorbent dosage, contact time, initial dye concentration and temperature were evaluated. Pseudo-first-order and pseudo-second-order kinetic models were tested to fit adsorption kinetic data. The equilibrium data were analyzed using Langmuir and Freundlich isotherm models.

EXPERIMENTAL

Materials

All the necessary chemicals used in this study were of analytical grade. MB and MG were provided by Sigma-Aldrich Chemicals and were used without further purification. HNO_3 (65%) was purchased from Sharlau (Spain) and NaOH from Merck (Germany). The chemical formula and some other specific characteristics of these dyes are summarized in Table 1.

Preparation of the adsorbents

Maize corncobs (locally obtained) were repeatedly washed with distilled water to remove dirt particles and were dried

Table 1 | Physicochemical characteristics of used dyes

Name	Molecular structure	M_W (g/mol)	λ_{max} (nm)
MB (Basic blue 9)	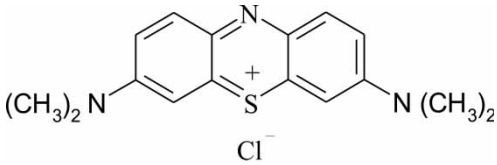	319.85	661
MG (Basic green 4)	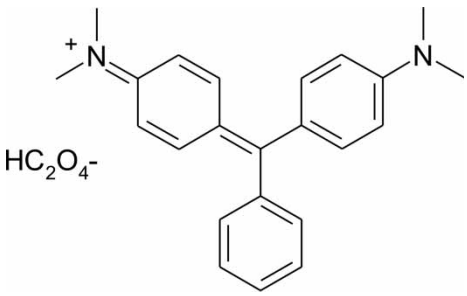	329.5	621

at 70 °C for 24 h. The dried corncobs were then powdered using a domestic mixer to particles of less than 160 μm in size. Ten g of the obtained raw maize corncobs (RMC) powder were carbonized at 500 °C for 2 h under nitrogen atmosphere. The obtained char was impregnated with phosphoric acid at a phosphoric acid to RMC ratio of 2.5 g/g for 6 h, followed by the removal of excess solution and overnight drying at 110 °C. The sample was further activated at 450 °C for 2 h. Subsequently, the cooled sample was repeatedly washed via hot deionized water to remove free phosphoric acid, tar, fines, and leachable matter followed by overnight drying at 110 °C. The obtained powder was powdered using a domestic mixer and sieved in particles of size lower than 125 μm using a normalized sieve. The obtained activated carbon was called AMC.

Characterization

The functional groups present at the surface of the RMC and AMC adsorbents were identified by FT-IR in the range of 4,400–400 cm^{-1} using a SCOTECH-SP-1 spectrophotometer. The samples were mixed with oven-dried spectroscopic grade KBr and pressed into a disk. XRD patterns were obtained using a Philips PW 1710 diffractometer equipped with a monochromatic Cu-Kα (1.541874Å). The diffraction patterns were recorded between 10 and 70 (2θ) degrees. The morphological characteristics of the RMC and AMC were analyzed by SEM using a FEI Quanta 200 model. A small amount of each sample was finely powdered and mounted directly on to an aluminum sample holder using a two-sided adhesive carbon model. The point of zero charge (pH_{PZC}) was determined by the pH drift method according to the method proposed by Noh & Schwarz (1989). The pH of NaCl aqueous solution (50 mL at 0.01 mol/L) was adjusted to successive initial values in the range of 2.0–12.0 by addition of HNO_3 (0.1 N) and/or NaOH (0.1 N). Moreover, 0.05 g of each adsorbent was added and stirred for 6 h. The final pH was measured and plotted against the initial pH. The pH_{PZC} was determined at the value for which $pH_{final} = pH_{initial}$.

Batch adsorption experiments

Adsorption experiments were performed in a series of 100 mL beakers containing the desired weight of each adsorbent and 50 mL of the dye solution at the desired concentration. These experiments were carried out at a constant agitation speed of 500 rpm by varying the pH of solution from 2 to 12, adsorbent dosage from 0.25 to 6 g/L, contact time from 5 to 300 min, initial dye concentration from 20 to 200 mg/L, and temperature from 10 to 50 °C. The solution pH was adjusted by adding NaOH (0.1 N) or HNO_3 (0.1 N) and measured by a sensION+ PH31 pH meter. The temperature was controlled using a thermostatically controlled incubator.

After each adsorption experiment was completed, the solid phase was separated from the liquid phase by centrifugation at 3,000 rpm for 10 min. Determination of the concentration of the dyes was carried out by spectrophotometric analysis in the visible range at the wavelength of maximum absorption of each dye (Table 1). The adsorbed quantity was calculated using the following equation:

$$q = \frac{(C_0 - C)}{R} \quad (1)$$

and the fading percentage/removal efficiency/adsorption efficiency:

$$\%\ \text{Removal} = \frac{(C_0 - C)}{C_0} * 100 \quad (2)$$

where q (mg/g) is the adsorbed quantity, C_0 (mg/L) is the initial dye concentration, C (mg/L) is the dye concentration at a time t, and R (g/L) is the mass of adsorbents per liter of solution.

RESULTS AND DISCUSSION

FT-IR analysis of the adsorbents

Figure 1 shows the FT-IR spectra of RMC and AMC. The spectra of the RMC sample shows a broad and strong band present between 3,600 and 3,200 cm^{-1}, which can be assigned to the O–H stretching mode of hydroxyl groups and adsorbed water (Yakout & Sharaf El-Deen 2012). The position and asymmetry of this band at lower wave numbers indicate the presence of strong hydrogen bonds (from carbonyls, phenols, or alcohols). After activation, this band was separated into three more resolute bands; two bands at around 3,300 and

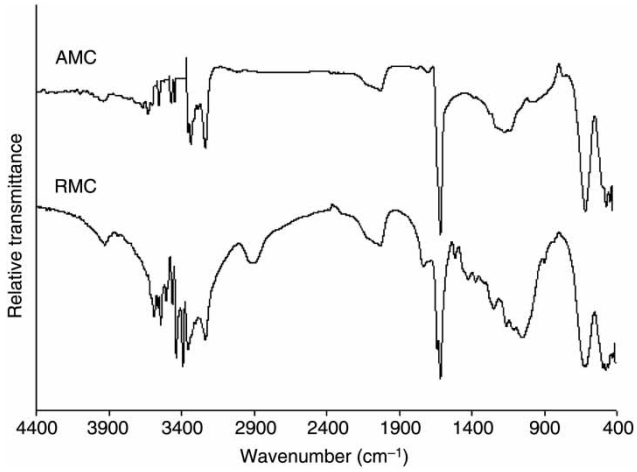

Figure 1 | FT-IR spectra of RMC and AMC adsorbents.

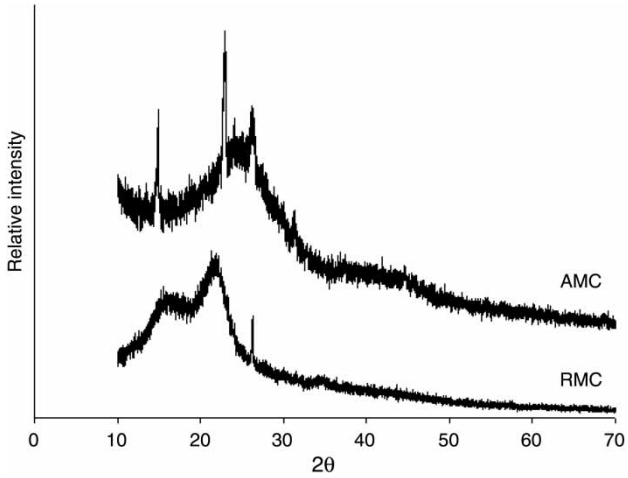

Figure 2 | XRD patterns of RMC and AMC samples.

3,250 cm^{-1} are ascribable to vibrations of hydroxyl groups, whereas the position of the band for non-bonded alcohols, phenols, and carboxylic acids is usually around 3,500 cm^{-1}. The band at 2,852 cm^{-1} for the raw corncob and not on activated corncob corresponds to the presence of $-CH_2$ stretching of aliphatic groups. The bands at 1,630 cm^{-1} are characteristic of C = O stretching vibrations of ketones, aldehydes, lactones, or carboxyl groups. These bands become finer in the activated corncob. The bands between 1,590 and 1,400 cm^{-1} are usually ascribed to C = C vibrations, although some overlapping can be found with (O-H) around 1,450 cm^{-1}. The bands about 1,030 cm^{-1} show the C–O–C stretching (alcohols, ethers, or phenols) and O–H deformation (Foo & Hameed 2011). These bands decreased by activation process as compared to the raw material.

XRD

The XRD patterns of RMC and AMC are shown in Figure 2. The XRD patterns of RMC exhibit broad peaks at $2\theta = 17^{\circ}$ indicating the amorphous part (i.e., cellulose, hemicellulose, and lignin) and at about $2\theta = 22.5^{\circ}$ denoting the partially crystallized portion of cellulose. The XRD patterns exhibit defined peaks and the absence of a broad peak in AMC reveals the predominantly amorphous structure of activated carbon. However, the occurrence of broad peaks at around $2\theta = 17^{\circ}$, 22.5°, and 26° that are related to the (101) and (002) show signs of formation of a carbonaceous crystalline structure, and that results in better layer alignment (Liou & Wu 2009). This feature is evident because the samples have a turbostratic structure. This type of pattern is known to be characteristic of the carbon states described as clusters made of small fragments of graphene layers plus a certain amount of disorganized carbon.

Morphology of the adsorbents

SEM photographs of RMC and AMC are shown in Figure 3. The figure reveals significant differences between the surface morphology of the RMC and the prepared activated carbon (AMC). From the figure the absence of any well-defined pores on the surface of raw material can be seen. After activation, the pores wall were opened and the surface became smooth with many different size and shape cavities. The H_3PO_4 impregnation and activation temperature are effective in creating well-developed pores on the surface of the AMC. These new pores are formed due to the reaction between carbon and the activating agent. The development of porous structure results from the decomposition of the sample matrix by the impregnation followed by evaporation of tars during the heat treatment. The prepared activated carbon will have large adsorption capacity due to high porosity.

pH point of zero charge

The pHs of zero charge (pH_{PZC}) of the adsorbents were found to be 6 and 3.5, respectively, for RMC and AMC. This result indicates that the adsorbents acquire a positive charge below a pH of 6 and 3.5, respectively, for RMC

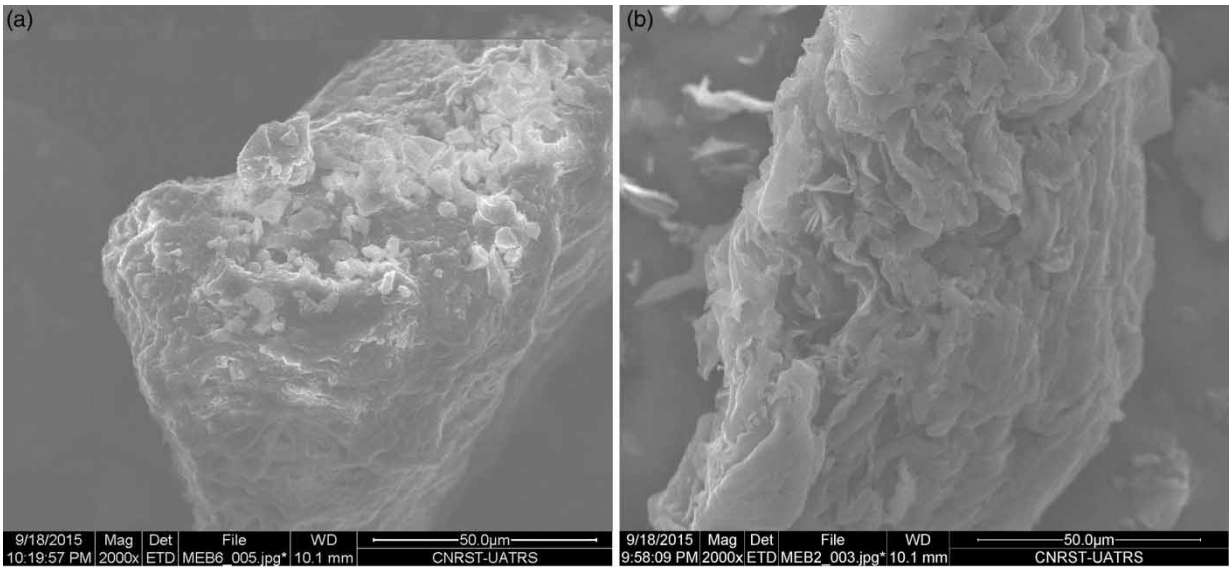

Figure 3 | SEM images of RMC (a) and AMC (b).

and AMC. Above these points, there is a net negative charge on the cell surface and the ionic state of functional groups at the surface of the adsorbents such as carboxyl, phosphoryl, sulfhydryl, and hydroxyl.

Effect of adsorbent dosage (R)

Figure 4 shows the effect of adsorbent dosage on the removal efficiency for MB and MG. The figure indicates that the adsorption yield increases with the increase in the adsorbent dosage and stabilizes at high adsorbent dosage. For RMC, the adsorption efficiency increased from 29.75 to 94.41% for MB and from 24.90 to 92.11% for MG when the adsorbent dosage increased from 0.25 to 4 g/L. For the AMC, the adsorption efficiency increased from 32.95 to 99.98% for MB and from 40.23 to 94.48% for MG when the adsorbent dosage was increased from 0.25 to 1 g/L. The observed enhancement in adsorption yield with increasing adsorbent dosage could be due to an increase in the number of possible binding sites and surface area of the adsorbents. A further increase in adsorbent dosage over 1 g/L for AMC and 4 g/L for RMC did not lead to a significant improvement in the adsorption yield. This may be due to the decrease in driving force for mass transfer at low concentration of dyes in solution (Barka *et al.* 2011a).

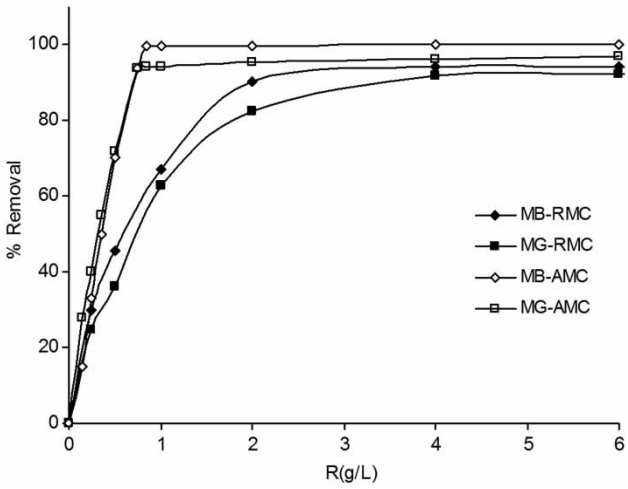

Figure 4 | Effect of adsorbent dosage on the removal of MB and MG by RMC and AMC: $C_0 = 100$ mg/L, contact time = 120 min, initial pH, $T = 25$ °C.

Effect of pH on the adsorption

Solution pH is a significant parameter which affects the dye adsorption process. It alters the surface charge of the adsorbents, the ionization state of dyes, as well as the structure of the dye molecules (Ai *et al.* 2011). Changes observed in the adsorption of MB and MG by RMC and AMC as a function of solution pH are presented in Figure 5. The figure indicates that as the pH increases, the adsorption

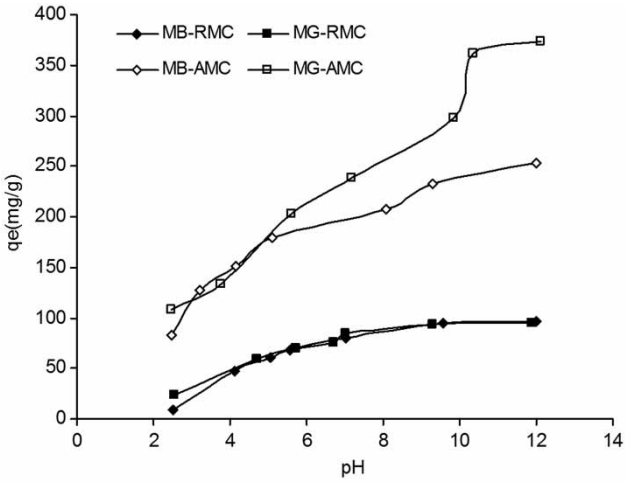

Figure 5 | Effect of solution pH on adsorption of MB and MG on RMC and AMC: $C_0 = 100$ mg/L, contact time = 120 min, $R = 1$ g/L for RMC and 0.25 g/L for AMC, $T = 25$ °C.

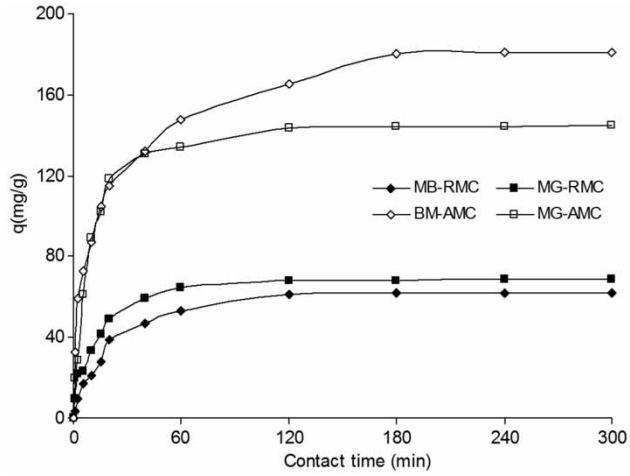

Figure 6 | Kinetics of MB and MG adsorption by RMC and AMC: $C_0 = 100$ mg/L, $R = 1$ g/L for RMC and 0.25 g/L for AMC, pH = initial solution pH, $T = 25$ °C.

capacities increase. This result may be due to a change in surface charge of both the dyes' molecules and functional groups of adsorbent. The pHs of zero charge (pH_{PZC}) of the adsorbents were found to be 6 and 3.5, respectively, for RMC and AMC. The pH_{PZC} values indicate that the adsorbents acquire a positive charge below a pH of 6 and 3.5, respectively for RMC and AMC. At pH values above this point, there is a net negative charge on the cell surface and the ionic state of functional groups such as carboxyl, phosphoryl, sulfhydryl, hydroxyl, and amino. Consequently, the adsorbent–adsorbate interactions for the cationic dyes become progressively significant for larger pH values. We can conclude from this result that the negative surface charge of the activated carbon becomes greater with increasing pH.

Adsorption kinetics

The kinetic parameters, which are supportive for the prediction of adsorption rate and equilibrium time, provide important information for designing and modeling of the adsorption processes (Sivarajasekar & Baskar 2014a). The results of the study of the influence of contact time on the adsorption of MB and MG are presented in Figure 6. According to this figure, the adsorption rate increases rapidly at the beginning of the process and becomes slow with the increase in the contact time until equilibrium is reached. The equilibration times were found to be 120 min for RMC and 180 min in the case of AMC. In order to characterize the kinetics involved in the process of adsorption, pseudo-first-order and pseudo-second-order rate equations were proposed and the kinetic data were analyzed based on the regression coefficient (r^2) and the amount of dye adsorbed per unit weight of each adsorbent.

The first-order rate expression of Lagergren based on solid capacity is generally expressed as follows (Lagergren 1898):

$$\frac{dq}{dt} = k_1 (q_e - q) \tag{3}$$

Integrating this equation for the boundary conditions $t = 0$ to $t = t$ and $q = 0$ to $q = q_t$, Equation (3) becomes:

$$q = q_e(1 - e^{-k_1 t}) \tag{4}$$

where q_e and q (both in mg/g) are, respectively, the amounts of metal adsorbed at equilibrium and at any time t (min), and k_1 (1/min) is the rate constant of adsorption.

In contrast, the pseudo-second-order kinetic equation is based on the adsorption capacity which may be expressed in the form (Ho & Mckay 1999):

$$\frac{dq}{dt} = k_2 (q_e - q)^2 \tag{5}$$

Integration of conditions with similar limits for the following equation gives:

$$q = \frac{k_2 q_e^2 t}{1 + k_2 q_e t} \quad (6)$$

where k_2 (g/mg min) is the rate constant of pseudo-second-order adsorption.

Parameters of the pseudo-first-order and pseudo-second-order models were estimated with the aid of nonlinear regression. The obtained data and the correlation coefficients, r^2, are given in Table 2.

The table shows that the correlation coefficients for the pseudo-second-order kinetic model are closer to one than those of the Lagergren first order. From these results the adsorption can be estimated more appropriately by the pseudo-second-order kinetic model. These results reveal that boundary layer resistance was not the rate limiting step (Ho & Mckay 1998). The rate of dye adsorption may be controlled largely by a chemisorption process, in conjunction with the chemical characteristics of the adsorbents and the dyes (Eren & Acar 2006).

Equilibrium sorption

To optimize the design of an adsorption system for the removal of solutes by adsorbents, it is important to establish the most appropriate correlation for the equilibrium curves. Adsorption isotherm provides valuable information such as equilibrium sorption capacity and certain constants whose values express the surface properties and affinity of the adsorbent (Sivarajasekar & Baskar 2014b). Figure 7 represents the adsorption isotherms for MB and MG on RMC and AMC. The results show that the absorbed amount increases with the increase of the equilibrium concentration of the dye. This increase may be due to the high driving force for mass transfer. The isotherms forms were of the type H for RMC and L for AMC in Giles' classification (Giles *et al.* 1974). In this study, the models of Langmuir and of Freundlich were used to describe the adsorption equilibrium.

Langmuir model

The most commonly used model is the Langmuir model (Langmuir 1918). The initial assumptions are that the solid adsorbent has a limited adsorption capacity, all active sites are identical, they can adsorb only one solute molecule (monolayer adsorption), and that there is no interaction between the adsorbed molecules. It means that once a dye molecule occupies a site, no further adsorption can take place on this site (Barka *et al.* 2012). The mathematical equation of Langmuir isotherm is expressed as follows:

$$q_e = \frac{q_m K_L C_e}{1 + K_L C_e} \quad (7)$$

where q_e (mg/g) is the adsorbed amount at equilibrium, C_e (mg/L) is the equilibrium dye concentration (mg/L), K_L is Langmuir equilibrium constant (L/mg), and q_m the Langmuir maximum adsorption capacity (mg/g).

Freundlich model

The simple empirical Freundlich model is most commonly used. It is considered to be applicable to many cases, particularly in the case of multilayer adsorption interaction

Table 2 | Kinetic parameters for the adsorption of MB and MG onto RMC and AMC

			Pseudo-first-order			Pseudo-second-order		
Adsorbent	**Dye**	q_{exp} (mg/g)	q_e (mg/g)	k_1 (L/min)	r^2	q_e (mg/g)	k_2 (g/mg min)	r^2
RMC	MB	61.20	60.82	0.0440	0.988	67.50	0.00840	0.992
	MG	67.97	66.97	0.0713	0.969	71.95	0.00147	0.983
AMC	MB	180.53	166.44	0.0733	0.905	179.27	0.00062	0.960
	MG	143.97	140.22	0.0989	0.991	150.42	0.00096	0.997

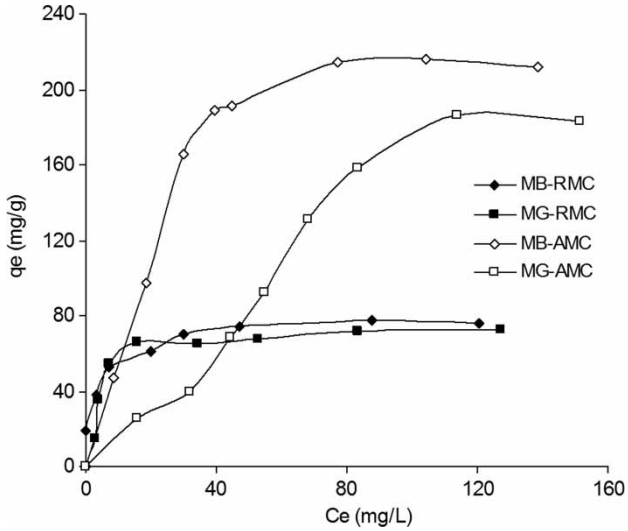

Figure 7 | Adsorption isotherms of MB and MG onto RMC and AMC: $R = 1$ g/L for RMC and 0.25 g/L for AMC, pH = initial solution pH, $T = 25$ °C, contact time = 120 min.

between the adsorbed molecules (Freundlich 1906). The Freundlich model equation is given as:

$$q_e = K_F C_e^{1/n} \quad (8)$$

where k_F ($mg^{1-1/n}/g/L^n$) is the Freundlich constant and n is the heterogeneity factor. The K_F value is related to the adsorption capacity; while 1/n value is related to the adsorption intensity.

Analysis of adsorption isotherms

The constants that characterize each of the above cited models were determined by nonlinear regression analysis. The obtained values are given in Table 3. The correlation coefficients (r^2) are also presented in this table. The table indicates that the best correlation to experimental results was obtained with the Langmuir model. The maximum monolayer adsorption capacities were 76.42 and 313.63 mg/g for the MG in the case of RMC and AMC. 75.27 and 271.19 mg/g for the MB in the case of RMC and AMC, respectively. These results indicate that activation of the corncob increases extremely the adsorption of MB and MG. The activation of maize corncob boosts four times the adsorption performance for the selected dyes.

In fact, another study based on various processes for the activation of corncob indicated little efficiencies for the adsorption of methyl orange (Hou *et al.* 2013). For further comparison with other materials, sorption capacities of MB and MG by several adsorbents studied in the literature are summarized in Table 4. It is obvious that RMC and AMC present greater sorption efficiencies than most organic and inorganic adsorbents previously studied. This study suggests that the RMC and AMC were more promising for an effective adsorption of MB and MG.

Effect of temperature

Figure 8 represents the variation of adsorbed amounts based on the temperature of the solution. From the figure we notice that the change in temperature has practically no influence on the adsorption efficiency. The observed trend could be due to the nature of the adsorbent particles. Increasing the temperature is known to increase the rate of the diffusion of molecules across the external boundary layer and the internal pores of the adsorbent particles, owing to the decrease in the viscosity of the solution. Therefore, changing temperature will change the equilibrium capacity of the adsorbent for a particular adsorbate.

Table 3 | Model isotherm constants for the adsorption of MB and MG onto RMC and AMC

	Langmuir				Freundlich		
Dye	**Adsorbent**	**q_m (mg/g)**	**K_L (L/mg)**	**r^2**	**K_F ($mg^{1-1/n}/g/L^n$)**	**n**	**r^2**
MB	RMC	75.27	0.355	0.978	43.24	5.589	0.945
	AMC	271.19	0.042	0.955	44.06	2.887	0.882
MG	RMC	76.42	0.210	0.941	28.96	4.791	0.848
	AMC	313.63	0.006	0.937	4.32	1.293	0.926

Table 4 | Sorption capacities (mg/g) for different adsorbents

Adsorbents	MB (mg/g)	MG (mg/g)	References
Coal fly ash	16.6	–	Wang *et al.* (2008)
Sewage sludge	114.9	–	Otero *et al.* (2003)
Modified montmorillonite	322.6	–	Wibulswas (2004)
Spent activated clay	127.5	–	Weng & Pan (2007)
Bagasse fly ash	–	42.18	Mall *et al.* (2005)
Coconut shell	–	214.63	Bello & Ahmad (2012)
Functionalized attapulgite	207.48	–	Zhang *et al.* (2015)
Sepiolite	57.38	–	Auta & Hameed (2012)
Aerobic granules	–	56.8	Sun *et al.* (2008)
Beech sawdust	–	83.21	Witek-Krowiak (2011)
Raw maize corncobs (RMC)	75.27	76.42	This study
AMC	271.19	313.63	This study

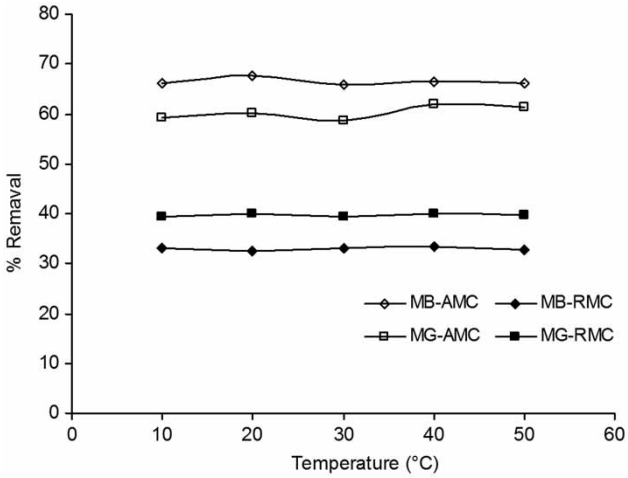

Figure 8 | Effect of temperature on the adsorption of MB and MG by RMC and AMC: $C_0 = 100$ mg/L, $R = 1$ g/L for RMC and 0.25 g/L for AMC, pH = initial solution pH.

CONCLUSIONS

This study has investigated MB and MG adsorption from an aqueous solution by RMC and H_3PO_4 AMC. The sorption characteristic has been examined using various sorption conditions. It was found that the sorption process was very rapid; the equilibrium time was obtained at 120 min for RMC and 180 min in the case of AMC. The sorption yield increases with the increase of sorbent dosage with an optimum at 1 g/L for RMC and 0.25 g/L for AMC. The optimum sorption was obtained at basic pH medium. Adsorption kinetics is better described by the pseudo-second-order model. The concentration of dye in the initial solution results in the increase of adsorption. The Langmuir model provides the best correlation of the experimental equilibrium data. The adsorption capacity was not influenced by temperature. Finally, these results show that AMC can be used as an efficient and economical adsorbent for the treatment of wastewaters containing synthetic dyes.

REFERENCES

Ai, L., Zhang, C. & Meng, L. 2011 Adsorption of methyl orange from aqueous solution on hydrothermal synthesized Mg–Al layered double hydroxide. *Journal of Chemical & Engineering Data* **56** (11), 4217–4225.

Auta, M. & Hameed, B. H. 2012 Modified mesoporous clay adsorbent 546 for adsorption isotherm and kinetics of methylene blue. *Chemical Engineering Journal* **198–199**, 219–227.

Barka, N., Assabbane, A., Aît Ichou, Y. & Nounah, A. 2006 Decontamination of textile wastewater by powdered activated carbon. *Journal of Applied Sciences* **6** (3), 692–695.

Barka, N., Ouzaouit, K., Abdennouri, M., El Makhfouk, M., Qourzal, S., Assabbane, A., Ait-Ichou, Y. & Nounah, A. 2012 Kinetics and equilibrium of cadmium removal from aqueous solutions by sorption onto synthesized hydroxyapatite. *Desalination and Water Treatment* **43** (1–3), 8–16.

Barka, N., Qourzal, S., Assabbane, A., Nounah, A. & Ait-Ichou, Y. 2011a Removal of Reactive Yellow 84 from aqueous solutions by adsorption onto hydroxyapatite. *Journal of Saudi Chemistry Society* **15** (3), 263–267.

Barka, N., Qourzal, S., Assabbane, A., Nounah, A. & Ait-Ichou, Y. 2011b Triphenylmethane dye, patent blue V, photocatalytic degradation on supported TiO_2: kinetics, mineralization and reaction pathway. *Chemical Engineering Communications* **198** (10), 1233–1243.

Bello, O. S. & Ahmad, M. A. 2012 Coconut (Cocos nucifera) shell based activated carbon for the removal of malachite green dye from aqueous solutions. *Separation Science and Technology* **47** (6), 903–912.

Brillas, E. & Martinez-Huitle, C. A. 2015 Decontamination of wastewaters containing synthetic organic dyes by electrochemical methods. An updated review. *Applied Catalysis B: Environmental* **166–167**, 603–643.

Chang, Y. M., Tsai, W. T. & Li, M. H. 2015 Characterization of activated carbon prepared from chlorella-based algal residue. *Bioresource Technology* **184**, 344–348.

Chen, Y., Zhai, S. R., Liu, N., Song, Y., An, Q. D. & Song, X. W. 2013 Dye removal of activated carbons prepared from NaOH-pretreated rice husks by low-temperature solution-processed carbonization and H_3PO_4 activation. *Bioresource Technology* **144**, 401–409.

Elmoubarki, R., Mahjoubi, F. Z., Tounsadi, H., Moustadraf, J., Abdennouri, M., Zouhri, A., El Albani, A. & Barka, N. 2015 Adsorption of textile dyes on raw and decanted Moroccan clays: kinetics, equilibrium and thermodynamics. *Water Resources and Industry* **9**, 16–29.

Ensuncho-Munoz, A. E. & Carriazo, J. G. 2014 Characterization of the carbonaceous materials obtained from different agro-industrial wastes. *Environmental Technology* **36** (5–8), 547–555.

Eren, Z. & Acar, F. N. 2006 Adsorption of Reactive Black 5 from an aqueous solution: equilibrium and kinetic studies. *Desalination* **194** (1–3), 1–10.

Foo, K. Y. & Hameed, B. H. 2011 Preparation and characterization of activated carbon from pistachio nut shells via microwave-induced chemical activation. *Biomass & Bioenergy* **35** (7), 3257–3261.

Freundlich, H. M. F. 1906 Over the adsorption in solution. *Journal of Physical Chemistry* **57**, 385–470.

Giles, C. H., Smith, D. & Huitson, A. 1974 A general treatment and classification of the solute adsorption isotherm I. Theoretical. *Journal of Colloid and Interface Science* **47** (3), 755–765.

Gokce, Y. & Aktas, Z. 2014 Nitric acid modification of activated carbon produced from waste tea and adsorption of methylene blue and phenol. *Applied Surface Science* **313**, 352–359.

Greluk, M. & Hubicki, Z. 2011 Efficient removal of Acid Orange 7 dye from water using the strongly basic anion exchange resin Amberlite IRA-958. *Desalination* **278** (1), 219–226.

Hazzaa, R. & Hussein, M. 2015 Adsorption of cationic dye from aqueous solution onto activated carbon prepared from olive stones. *Environmental Technology & Innovation* **4**, 36–51.

Herawan, S. G., Hadi, M. S., Ayob, Md. R. & Putra, A. 2013 Characterization of activated carbons from oil-palm shell by CO_2 activation with no holding carbonization temperature. *Scientific World Journal* **2013**, 1–6.

Ho, Y. S. & Mckay, G. 1998 The kinetics of sorption of basic dyes from aqueous solution by sphagnum mass peat. *Canadian Journal of Chemical Engineering* **76** (4), 822–827.

Ho, Y. S. & Mckay, G. 1999 Pseudo-second order model for sorption processes. *Process Biochemistry* **34** (5), 451–465.

Hou, X. X., Deng, Q. F., Ren, T. Z. & Yuan, Z. Y. 2013 Adsorption of Cu(2+) and methyl orange from aqueous solutions by activated carbons of corncob-derived char wastes. *Environmental Science and Pollution Research International* **20** (12), 8521–8534.

Isah, U., Abdulraheem, G., Bala, S., Muhammad, S. & Abdullahi, M. 2015 Kinetics, equilibrium and thermodynamics studies of C.I. Reactive Blue 19 dye adsorption on coconut shell based activated carbon. *International Biodeterioration and Biodegradation* **102**, 265–273.

Junior, O. P., Cazetta, A. L., Gomes, R. C., Barizão, E. O., Souza, I. P. A. F., Martins, A. C., Asefa, T. & Almeida, V. C. 2014a Synthesis of $ZnCl_2$-activated carbon from macadamia nut endocarp (*Macadamia integrifolia*) by microwave-assisted pyrolysis: optimization using RSM and methylene blue adsorption. *Journal of Analytical and Applied Pyrolysis* **105**, 166–176.

Junior, O. P., Cazetta, A. L., Souza, I. P. A. F., Bedin, K. C., Martins, A. C., Silva, T. L. & Almeida, V. C. 2014b Adsorption studies of methylene blue onto $ZnCl_2$-activated carbon produced from buriti shells (*Mauritia flexuosa* L.). *Journal of Industrial and Engineering Chemistry* **20** (6), 4401–4407.

Kanchi, S., Bisetty, K., Kumar, G. & Sabela, M. I. 2013 Robust adsorption of Direct Navy Blue-106 from textile industrial effluents by bio-hydrogen fermented waste derived activated carbon: equilibrium and kinetic studies. *Arabian Journal of Chemistry*. http://dx.doi.org/10.1016/j.arabjc.2013.11.050.

Karacetin, G., Sivrikaya, S. & Imamoglu, M. 2014 Adsorption of methylene blue from aqueous solutions by activated carbon prepared from hazelnut husk using zinc chloride. *Journal of Analytical and Applied Pyrolysis* **110** (1), 270–276.

Lagergren, S. 1898 About the theory of so-called adsorption of soluble substance Seven Vetenskapsakad. *HandBand* **24** (4), 1–39.

Langmuir, I. 1918 The adsorption of gases on plane surfaces of glass mica and platinum. *Journal of American Chemical Society* **40** (9), 1361–1403.

Li, Y., Zhang, X., Yang, R., Li, G. & Hu, C. 2016 Removal of dyes from aqueous solutions using activated carbon prepared from rice husk residue. *Water Science & Technology* **73** (5), 1122–1128. doi:10.2166/wst.2015.450.

Lin, S. H. & Peng, F. C. 1996 Continuous treatment of textile wastewater by combined coagulation, electrochemical oxidation and activated sludge. *Water Research* **30**, 587–592.

Liou, T. H. & Wu, S. J. 2009 Characteristics of microporous/mesoporous carbons prepared from rice husk under base- and acid-treated conditions. *Journal of Hazardous Materials* **171** (1–3), 693–703.

Mall, I. D., Srivastava, V. C., Agarwal, N. K. & Mishra, I. M. 2005 Adsorptive removal of malachite green dye from aqueous solution by bagasse fly ash and activated carbon-kinetic study and equilibrium isotherm analyses. *Colloids and Surfaces A: Physicochemical and Engineering Aspects* **264** (1), 17–28.

Morikawa, C. K. & Shinohara, M. 2016 Heterogeneous photodegradation of methylene blue with iron and tea or coffee polyphenols in aqueous solutions. *Water Science & Technology* **73** (8), 1872–1881.

Noh, J. S. & Schwarz, J. A. 1989 Estimation of the point of zero charge of simple oxides by mass titration. *Journal of Colloid and Interface Science* **130** (1), 157–164.

Otero, M., Rozada, F., Calvo, L. F., Garcia, A. L. & Moran, A. 2003 Kinetic and equilibrium modelling of the methylene blue removal from solution by adsorbent materials produced from sewage sludges. *Biochemical Engineering Journal* **15** (1), 59–68.

Patterson, P. 2012 The impact of environmental regulation on future textile products and processes. In: *The Global Textile and Clothing Industry* (R. Shishoo, ed.). The Textile Institute, Woodhead Publishing, Cambridge, pp. 20–54.

Ranjithkumar, V., Nizarul Hazeen, A., Thamilselvan, M. & Vairam, S. 2014 Magnetic activated carbon-Fe_3O_4 nanocomposites–synthesis and applications in the removal of acid yellow dye 17 from water. *Journal of Nanoscience and Nanotechnology* **14** (7), 4949–4959.

Rosa, J. M., Tambourgi, E. B., Santana, J. C. C., Araujo, M. D. C., Ming, W. C. & Trindade, N. 2014 Development of colors with sustainability: a comparative study between dyeing of cotton with reactive and vat dyestuffs. *Textile Research Journal* **84**, 1009–1017.

Rosa, J. M., Fileti, A. M. F., Tambourgi, E. B. & Santana, J. C. C. 2015 Dyeing of cotton with reactive dyestuffs: the continuous reuse of textile wastewater effluent treated by Ultraviolet/Hydrogen peroxide homogeneous photocatalysis. *Journal of Cleaner Production* **90**, 60–65.

Secondes, M. F. N., Naddeo, V., Belgiorno, V. & Junior, F. B. 2014 Removal of emerging contaminants by simultaneous application of membrane ultrafiltration, activated carbon adsorption, and ultrasound irradiation. *Journal of Hazardous Materials* **264**, 342–349.

Sivarajasekar, N. & Baskar, R. 2014a Adsorption of Basic Magenta II onto H_2SO_4 activated immature Gossypium hirsutum seeds: kinetics, isotherms, mass transfer, thermodynamics and process design. *Arabian Journal of Chemistry*. http://dx.doi.org/10.1016/j.arabjc.2014.10.040.

Sivarajasekar, N. & Baskar, R. 2014b Adsorption of basic red 9 on activated waste Gossypium hirsutum seeds: process modelling, analysis and optimization using statistical design. *Journal of Industrial and Engineering Chemistry* **20** (5), 2699–2709.

Sun, X. F., Wang, S. G., Liu, X. W., Gong, W. X., Bao, N., Gao, B. Y. & Zhang, H. Y. 2008 Biosorption of Malachite Green from aqueous solutions onto aerobic granules: kinetic and equilibrium studies. *Bioresource Technology* **99**, 3475–3483.

Titirici, M. M., White, R. J., Falco, C. & Sevilla, M. 2012 Black perspectives for a green future: hydrothermal carbons for environment protection and energy storage. *Energy & Environmental Science* **5** (5), 6796–6822.

Tounsadi, H., Khalidi, A., Abdennouri, M. & Barka, N. 2015 Activated carbon from *Diplotaxis Harra* biomass: optimization of preparation conditions and heavy metal removal. *Journal of the Taiwan Institute of Chemical Engineers* **59**, 348–358.

Vymazal, J. 2014 Constructed wetlands for treatment of industrial wastewaters: a review. *Ecological Engineering* **73** (1), 724–751.

Wang, S., Ma, Q. & Zhu, Z. 2008 Characteristics of coal Fly ash and adsorption application. *Fuel* **87** (15–16), 3469–3473.

Wang, Z., Xue, M., Huang, K. & Liu, Z. 2011 Textile dyeing wastewater treatment. *Advances in Treating Textile Effluent* (P. Hauser, ed.). InTech, doi: 10.5772/22670.

Weng, C. H. & Pan, Y. F. 2007 Adsorption of a cationic dye (methylene blue) onto spent activated clay. *Journal of Hazardous Materials* **144** (1–2), 355–362.

Wibulswas, R. 2004 Batch and fixed bed sorption of methylene blue on precursor and QACs modified montmorillonite. *Separation and Purification Technology* **39** (1–2), 3–12.

Witek-Krowiak, A. 2011 Analysis of influence of process conditions on kinetics of malachite green biosorption onto beech sawdust. *Chemical Engineering Journal* **171**, 976–985.

Yagub, M. T., Sen, T. K., Afroze, S. & Ang, H. M. 2014 Dye and its removal from aqueous solution by adsorption: a review. *Advances of Colloid and Interface Science* **209**, 172–184.

Yakout, S. M. & Sharaf El-Deen, G. 2012 Characterization of activated carbon prepared by phosphoric acid activation of olive stones. *Arabian Journal of Chemistry*. http://dx.doi:10.1016/j.arabjc.2011.12.002.

Zhang, Z., Wang, W. & Wang, A. 2015 Highly effective removal of Methylene Blue using functionalized attapulgite via hydrothermal process. *Journal of Environmental Science* **33**, 106–115.

Zhu, M. X., Lee, L., Wang, H. H. & Wang, Z. 2007 Removal of an anionic dye by adsorption/precipitation processes using alkaline white mud. *Journal of Hazardous Materials* **149** (3), 735–741.

Zylla, R., Sojka-Ledakowicz, J., Stelmach, E. & Ledakowicz, S. 2006 Coupling of membrane filtration with biological methods for textile wastewater treatment. *Desalination* **198** (1), 316–325.

First received 30 September 2016; accepted in revised form 9 December 2016. Available online 22 February 2017